The Temperature and Pressure Dependence of Vapor-Phase Photoassociation: Excimer Formation in 1-Azabicyclo[2.2.1]heptane. Evidence of Collision-Induced Dissociation

Arthur M. Halpern* and Ali Taaghol

Contribution from the Department of Chemistry, Northeastern University, Boston, Massachusetts 02115. *Received February 9, 1987*

Abstract: At ambient temperatures, the vapor-phase fluorescence spectrum of the cage amine 1-azabicyclo[2.2.1]heptane (ABCH) shows strong excimer emission (λ_{max} 380 nm), which is widely separated from the structured monomer fluorescence (ca. 256 nm). The ABCH vapor pressure is large enough to allow the quantitative measurement of both monomer and excimer fluorescence decay curves throughout four decades between 298 and 473 K. The photokinetics are examined within the context of a simple monomer/excimer scheme. Below 398 K, monomer decay curves are single exponential, indicating that excimer dissociation is too slow to measure. The temperature dependence of the photokinetic parameters reveals a negative temperature coefficient for the formation rate constant (i.e., −10 kJ/mol). On the basis of mean collision diameter of 9 Å, the excimer formation probability is ca. 0.12 at 298 K. Above 398 K, the data indicate that excimer dissociation is collisionally induced by ground-state molecules (rate constant 4.5×10^8 M^{-1} s^{-1} at 423 K). The zero-pressure-extrapolated values of the first-order dissociation rate constants are non-zero and do not show Arrhenius behavior. The temperature and pressure dependence of excimer formation and dissociation is discussed in terms of simple unimolecular rate theory. Data are compared with the binding energy of the ABCH excimer in the condensed phase. The photokinetic data are in general agreement with photostationary measurements carried out at constant ABCH vapor concentration.

The study of excimer (excited dimer) formation and dissociation in the vapor phase provides an opportunity to examine and characterize the reaction dynamics and energetics of a relatively simple reaction.[1] This process is the formation and dissociation of a weak bond (e.g., 40–50 kJ/mol) formed between two polyatomic molecules in the absence of solvent or medium effects. The absence of environmental effects allows, for example, the role and effectiveness of collisions in excimer formation *and* dissociation to be examined. With respect to the fission of the excimer into ground- and excited-state monomers, a question of interest is whether this process takes place unimolecularly, or bimolecularly, at moderate amine pressures (5–20 Torr). It might be expected that the excimer, a large polyatomic molecule (38 atoms, in the present study), would manifest the "fall off" in the observed first-order dissociation rate constant at relatively low pressures (i.e., below a few Torr).

In the case of the excimer in saturated cage amines, the excimer bond is postulated to be localized between the nitrogen atoms of the two amines that face each other.[2] Moreover, because of the Rydberg nature of the excited-state monomer from which this bound dimeric species is derived,[3] the association between the amines may be thought of in terms of a three-electron bond. Moreover, since the intermonomeric bond in the excimer is relatively weak, and presumably localized, it is of considerable interest to study the temperature dependence of the formation and dissociation dynamics in relation to other simple vapor-phase association reactions, as well as to excimer formation and emission in the condensed phase. Also, since the "reactive site" of the cage amine is also localized, it is interesting to determine the binary collision efficiency of excimer formation.

There have been relatively few studies of intermolecular photoassociation (excimer and exciplex formation and emission) in the vapor phase.[4,5] This is primarily because the temperatures required to sustain a sufficiently high vapor pressure (hence collision frequency) are so high that excimer (or exciplex) fluorescence cannot compete favorably with back dissociation. Hence the emission efficiencies of the excited complexes are often too small to permit quantitative photokinetic studies. Significant exceptions to this situation are provided by two saturated tertiary cage amines which have appreciable vapor pressures at ambient temperature. For example, 1-azabicyclo[2.2.2]octane (ABCO) was shown to undergo excimer formation and emission at ambient temperature.[4] Another cage amine, 1-azabicyclo[2.2.1]heptane (ABCH), also manifests excimer formation and emission at ambient vapor temperatures;[6] it is this latter compound that is used as a model for excimer formation in this study.

Experimental Section

1-Azabicyclo[2.2.1]heptane (ABCH) was obtained from Reilly Tarr and Chemical Corp. As received, this material was a low-melting solid; it was dried and purified as follows. Lithium aluminum hydride was added to a concentrated solution of the amine in 2-methylbutane. After bubbling ceased, the solvent was slowly evaporated and the remaining solid was sublimed under high vacuum. The product was stored under vacuum and was resublimed directly into the fluorescence cell sidearm immediately prior to measurements. The ABCH vapor pressure was measured with the use of a capacitance manometer (MKS Type 77). Between 259 and 290 K, the vapor pressure of ABCH follows the relation $\ln P_{vap}(\text{Torr}) = 20.43 - (5.31 \times 10^3)/T(\text{K})$. This expression was assumed to be valid over the temperature range used in this study, 263–318 K. Fluorescence spectra and lifetimes were measured in a 10.00 cm long cylindrical cell (3.0-cm diameter) constructed entirely of Suprasil (Hellma Cells, Inc.). A length of 1.0 cm (o.d.) tubing, closed at one end and separated from the cell body by 7.5 cm, served as a reservoir which contained the solid amine. The vapor pressure of the solid was controlled by the temperature of a small aluminum block into which the sidearm snugly fit. The block temperature was established by a thermoelectric module driven by a power supply and controlled by feedback from a thermistor imbedded in the block. Temperature stability was ca. ±0.2 K. The fluorescence cell was contained in an aluminum oven fitted with Suprasil windows and insulating material. Heating was affected by four

(1) Birks, J. B. *Rep. Prog. Phys.* **1975**, *38*, 903.
(2) Halpern, A. M.; Sternfels, R. J.; Ravinet, P. *J. Am. Chem. Soc.* **1977**, *99*, 169.
(3) (a) Robin, M. B. *Higher Excited States of Polyatomic Molecules*; Academic: New York, 1974; Vol. 1, pp 208–229. (b) Kawasaki, M.; Kasatani, K.; Sato, H.; Shinohara, H.; Nishi, N.; Ibuki, T. J. *Chem. Phys.* **1982**, *77*, 258.
(4) Halpern, A. M. *J. Am. Chem. Soc.* **1974**, *96*, 4392.
(5) (a) Itoh, M.; Hanashima, Y. *J. Am. Chem. Soc.* **1981**, *103*, 2371. (b) Itoh, M.; Hanashina, Y.; Wada, N.; Hanazaki, I. *Bull. Chem. Soc. Jpn.* **1983**, *56*, 1944. (c) Felker, P. M.; Syage, J. A.; Lambert, W. R.; Zewail, A. H. *Chem. Phys. Lett.* **1982**, *92*, 1.
(6) Halpern, A. M.; Frye, S. L.; Ko, J.-J. *Photochem. Photobiol* **1984**, *40*, 555.

0002-7863/87/1509-5986$01.50/0

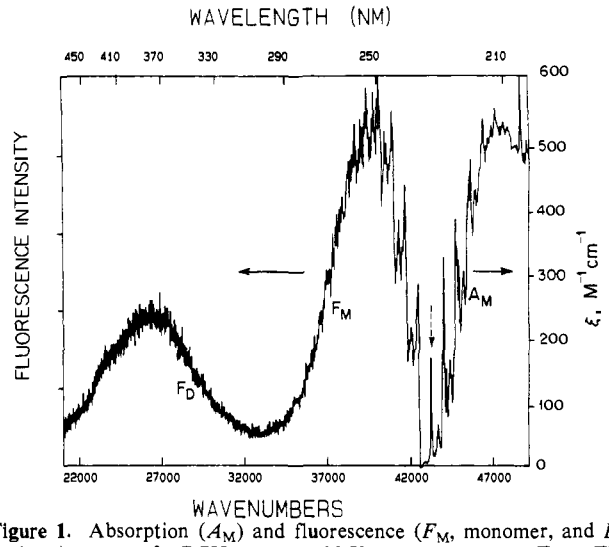

Figure 1. Absorption (A_M) and fluorescence (F_M, monomer, and F_D excimer) spectra of ABCH vapor at 298 K, vapor pressure 12 Torr. The vertical arrow denotes the 0–0 band at 231.6 nm. Excitation wavelength is 231 nm.

0.25 × 4 in. heating cartridges (Hotwatt) mounted symmetrically with respect to the cell. The oven temperature was controlled (±0.5 K) and monitored with a thermocouple-power supply (Omega Engineering 4001-JC). ABCH is evidently relatively thermally stable. There was no evidence of decomposition product(s) after the amine was confined to the cell at high temperatures (i.e., up to ~500 K) for several hours. In the photokinetic (photon counting) experiments, ABCH was exposed to very low light fluence; in the photostationary experiments which involved higher light intensities, exposure was minimized, and there was no evidence of photo/thermal decomposition. Fluorescence decay curves were obtained with use of a time-correlated photon-counting apparatus described elsewhere. Radiation from a D_2-filled (0.5 atm) flashlamp, operated at 30 kHz, was isolated by a 1/4-m Ebert-mount monochromator (Jarrel-Ash) having a band pass of 3.2 nm. Emission was detected through interference filters (monomer at 256 nm, and excimer at 380 nm), having a band pass of 10 and 8 nm, respectively (Corion Corp.). Because of the long time scale required in these studies (e.g., up to 1.4 s), the excitation flash pulse was deliberately widened in order to minimize the interference caused by residual emission in the tail of the deuterium discharge at long times (at ca. 1–2 s). This measure was particularly important because fluorescence intensity was measured over a dynamic range of four decades and was achieved by adding a 20-pF capacitor (ceramic, 7 kV) to the flashlamp anode. With this arrangement, the half-width of the lamp was about 3 ns. The low optical density of the sample and the often weak emission from the sample (especially excimer) required acquisition times of typically 2 h for a pair of decay curves. Fluorescence decay curves (often exhibiting two components) were analyzed with the aid of a reconvolution program installed on a dedicated LSI 11/23 microcomputer.[6] The uncertainties in the photokinetic parameters (including reproducability) are ~1% for the short-lived component, ~1.8% for the long-lived component, and ~3% for the amplitude ratio (below 473 K), and ~8% above 473 K. Emission spectra were obtained with a dc fluorimeter employing a 60-W D_2 lamp. The ABCH vapor pressure was adjusted by controlling the sidearm temperature in order to keep the vapor concentration in the fluorescence cell constant throughout the steady-state experiment. ABCH was assumed to follow the ideal gas law.

Results and Discussion

ABCH is an excellent model for studying the temperature and self-pressure effects on the dynamics of photoassociation. Its vapor pressure is appreciable at ambient temperature (e.g., 13.6 Torr at 298 K, see Experimental Section), and this provides a large enough collision frequency for excimer emission to be easily observed. Moreover at higher temperatures where excimer dissociation diminishes its fluorescence yield, the accessibility of higher vapor concentrations partially offsets this problem. Thus the intrinsic monomer and excimer fluorescence efficiencies are both adequate for quantitative studies. Figure 1 shows a portion of the absorption spectrum and the monomer and excimer emission spectra of ABCH at ambient vapor temperature. The 0–0 bands of the $S_1 \leftrightarrow S_0$ ($3s \leftrightarrow n_N$) transitions overlap at 231.6 nm. The

Scheme I

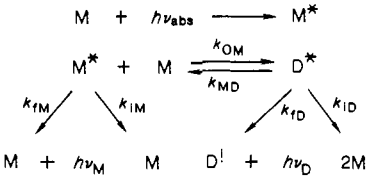

$S_1 \leftarrow S_0$ transition is structured and reveals a distinct progression in 725 cm^{-1}, which in analogy with ABCO can be assigned as a cage-distorting mode (cf. 625 cm^{-1}, for ABCO).[7] The sharp feature at 205.8 nm is the 0–0 band of the $S_2 \leftarrow S_0$ ($3p \leftarrow n_N$) transition(s).

Fluorescence is also highly structured, especially on the high-energy and of the spectrum. The Franck-Condon maximum at ca. 254 nm is considerably displaced from that of the absorption spectrum (ca. 213 nm) which, even accounting for the overlap with the stronger $S_2 \leftarrow S_0$ transition, manifests a large Stokes's shift (7580 cm^{-1}) indicating considerable displacement between the equilibrium positions of the N-bridgehead cage structures in the lower and upper electronic states. Such geometry changes are typical of saturated amines, both caged and acyclic.[8]

The excimer emission, broader than the monomer spectrum and totally unstructured, is considerably displaced to lower energies (λ_{max} = 380 nm). This large separation facilitates monitoring the emission from the two species separately. The sizable monomer–excimer emission gap (13 050 cm^{-1}, 156 kJ) indicates an appreciable value for the sum of the excimer binding energy and (ground state) repulsion energy.[9] In fact, the binding energy of ABCH in *n*-hexadecane solution has been reported to be 51.0 kJ,[9] implying a close approach of the two amine moieties in the excimer. The rather large activation energy to dissociation indicated by this value requires that measurements of excimer fission be carried out at elevated temperatures where the dissociation rate competes favorably with intrinsic excimer relaxation (e.g., 4 × 10^6 s^{-1}). The strategy pursued in this study was to measure the temperature dependence of the decay kinetics of ABCH monomer and excimer after nanosecond pulse excitation at 231 nm and to determine the formation and dissociation rate constants and their temperature coefficients. The 231-nm wavelength is very close to the 0–0 band of the $S_1 \leftarrow S_0$ transition and was chosen as the excitation wavelength to avoid the complications that arise when (monomer) vibrational relaxation concomitant with excimer formation when higher excitation energies are used.[11] Although lower fluorescence signal strengths are observed because of the smaller optical density at this wavelength (relative to higher energies, see Figure 1), it is desirable to prevent the initially formed monomer from being too vibrationally excited.

For ABCH vapor temperatures between 298 and ca. 363 K, excited monomer decay, monitored at 256 nm, follows single exponential decay for 3–4 decades of intensity, the range usually spanned in these experiments. Excimer decay, followed at 380 nm, exhibits biexponential decay, the shorter lived component closely agreeing with that of the monomer decay curve. Significantly, this short-lived component has an amplitude equal and opposite to that of the long-lived component. For ABCH vapor at 343 K and a concentration of 1.73 × 10^{-4} M, for example, the monomer and excimer decay curves are

$$I_{fM}(t) = \exp(-17.5 \pm 0.2)t$$

and

$$I_{fD}(t) = \exp(-3.92 \pm 0.07)t - \exp(-17.5 \pm 0.2)t$$

(7) Halpern, A. M.; Roebber, J. L.; Weiss, K. *J. Chem. Phys.* **1968**, *49*, 1348.
(8) Halpern, A. M.; Ondrechen, M. J.; Ziegler, L. D. *J. Am. Chem. Soc.* **1986**, *108*, 3907.
(9) Birks, J. B. *Photophysics of Aromatic Molecules*; Wiley-Interscience: London, 1971; pp 325–327.
(10) Halpern, A. M.; Nosowitz, M.; Ramachandran, B. R. *J. Photochem.* **1980**, *12*, 167.
(11) Halpern, A. M.; Taaghol, A., unpublished results.

Table I. Summary of the Rate Constants for the ABCH Monomer/Excimer System

T (K)	k_M[a]	k_{DM}[b]	Y^0[a]	$k_{MD}{}^0$[c]	$k_{MD}{}'$[d]	k_D[a]
298	7.3 ± 0.1	6.9 ± 0.1				3.7 ± 0.1
318	7.7 ± 0.1	6.4 ± 0.1				3.8 ± 0.1
343	9.8 ± 0.1	4.6 ± 0.1				3.9 ± 0.1
363	8.7 ± 0.1	3.5 ± 0.07				3.8 ± 0.1
398	10.2 ± 0.2	2.5 ± 0.05	4.0 ± 0.2	0.8 ± 0.04	2.0 ± 0.5	3.6 ± 0.2
423	11.5 ± 0.3	2.1 ± 0.04	4.7 ± 0.2	1.0 ± 0.05	4.5 ± 0.4	4.6 ± 0.3
453	13.1 ± 0.3	2.0 ± 0.04	6.0 ± 0.3	1.3 ± 0.05	4.5 ± 0.4	5.8 ± 0.4
473	13.0 ± 0.3	2.5 ± 0.05	6.9 ± 0.3	2.0 ± 0.1	4.5 ± 0.4	6.7 ± 0.5
493	13.7 ± 0.3	2.4 ± 0.05	8.8 ± 0.4	*e*	*e*	(8.8)

[a] 10^6 s^{-1}. [b] 10^{10} M^{-1} s^{-1}. [c] 10^5 s^{-1}. [d] 10^8 M^{-1} s^{-1}. [e] These data are unreliable at this temperature.

where t is in μs. The good agreement between the decay constants of the monomer and excimer, as well as the precision of the −1 ratio of the two components in the excimer decay curve, suggests that the ABCH vapor system is amenable to the simple monomer/excimer kinetic scheme shown in Scheme I, where M denotes the monomeric amine and D^1 represents the unstable ground-state dimer having the equilibrium excimer structure. Subsequent to delta pulse excitation, the time dependencies of excited monomer, M*, and excimer, D*, follow the well-known decay laws[12]

$$I_{fM}(t) = \exp(-\lambda_1 t) + A \exp(-\lambda_2 t) \quad (1)$$

and

$$I_{fD}(t) = \exp(-\lambda_1 t) - \exp(-\lambda_2 t) \quad (2)$$

where the time constants and relative amplitude A are functions of the four rate constants indicated above, i.e.

$$2\lambda_{1,2} = (X + Y) \mp \{(X - Y)^2 + 4k_{DM}k_{MD}[M]\}^{1/2} \quad (3)$$

where X, Y, and A are defined as

$$X = k_M + k_{DM}[M] \qquad Y = k_D + k_{MD} \quad (4)$$

$$A = (X - \lambda_1)/(\lambda_2 - X) \quad (5)$$

k_M and k_D are the intrinsic decay constants of excited monomer and excimer, each containing radiative and nonradiative components

$$k_M = k_{fM} + k_{iM} \text{ and } k_D = k_{fD} + k_{iD} \quad (6)$$

X and Y are obtained from the measured values of λ_1, λ_2, and A through the relations

$$X = (A\lambda_2 + \lambda_1)/(A + 1) \qquad Y = \lambda_1 + \lambda_2 - X \quad (7)$$

and the four rate constants are obtained from analyzing the pressure dependence of λ_1, λ_2, and X. The uncertainties in λ_1, λ_2, and A are discussed in the Experimental Section. For example, k_M and k_{DM} are obtained from the intercept and slope, respectively, of X vs [M]. The analysis of k_D and k_{MD} will be discussed below.

From eq 1 the excited monomer is predicted to undergo double exponential decay, the longer lived component representing (in this case) dissociative "feed back" from the excimer. The fact that single-exponential decay is observed below ca. 363 K can be ascribed to the very small values of k_{DM} in this temperature regime. Double exponential decay curves are observed above ca. 398 K for the ABCH monomer (for a sensitivity of 4 decades).

Because the objective of this study was to examine the dissociation dynamics of ABCH, as well as the association kinetics (which can be probed in the absence of the long-lived component in the monomer decay curves), studies had to be carried out at higher temperatures. Accordingly, decay curves of excimed monomer and excimer were obtained between 298 and 473 K. At the higher temperatures in this range, the count rate at 380 nm was too low to permit excimer decay curves of adequate accuracy to be acquired. Nevertheless, under these circumstances, the double exponential monomer decay curves observed allowed the extraction of the desired rate constants (see below).

(12) Reference 9, pp 304–307.

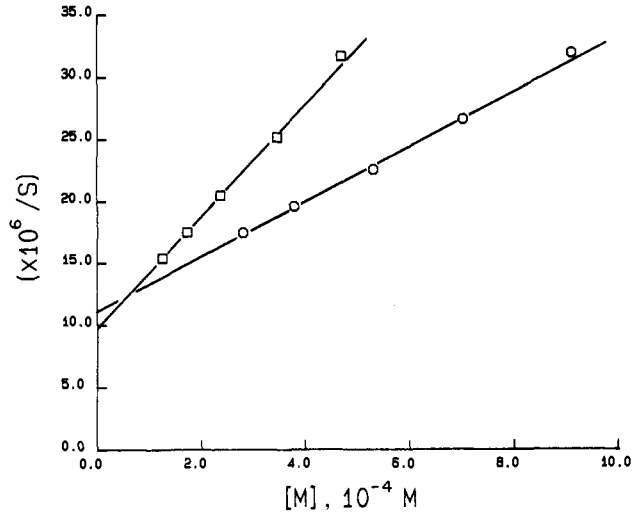

Figure 2. (□) Plot of λ_2 vs. ABCH vapor concentration at 343 K. (○) Plot of X vs. ABCH vapor concentration at 423 K.

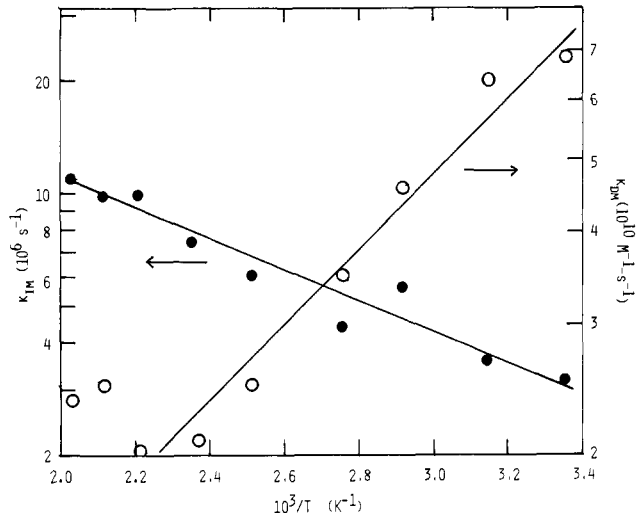

Figure 3. (●) Arrhenius plot of k_{iM}. (○) Arrhenius plot of k_{DM}.

Excimer Formation Dynamics

In the low-temperature regime where excimer dissociation is too slow to be determined with these experimental methods, (3) predicts that $\lambda_2 \sim X$, and thus plots of λ_2 vs. [M] should be linear. This is observed below 398 K, and an example is shown in Figure 2 for ABCH vapor at 343 K. In the high-temperature regime, where the monomer decays biexponentially (allowing a value of A to be determined), X vs. [M] is expected to be linear, and such is the case. Figure 2 also shows X vs. [M] at 423 K. These plots provide values of k_M and k_{DM} as intercepts and slopes, respectively. Throughout the entire temperature range covered in this study (298–473 K), excellent linear plots of X (or λ_2) vs. [M] were obtained (for $2.3 \times 10^{-4} < [M] < 1.2 \times 10^{-3}$ M). The values of k_M and k_{DM} thus obtained are presented in Table I. It thus appears that the quenching of excited monomer by ground state

to form the emissive excimer is a bimolecular process. The results indicate that both k_M and k_{DM} are weakly temperature dependent. An Arhenius plot of k_{DM} is shown in Figure 3. The value of k_M at 298 K is 7.3×10^6 s^{-1} and compares with 2.75×10^6 s^{-1} for its homologue, ABCO.[4]

An Arrhenius plot of k_M between 298 and 473 K is somewhat curved; this is not unexpected in view of the fact that it is a composite rate constant ($k_{fM} + k_{iM}$). The quantum efficiency of monomer fluorescence is not known, thus k_M cannot be partitioned into its components. Qualitative information can be obtained, however, by estimating k_{fM} from the integrated absorption strength of the $S_1 \leftarrow S_0$ transition and the mean inverse cube of the fluorescence frequency.[13] This calculation for ABCH leads to a value for k_{fM} of 3×10^6 s^{-1}, and thus suggests a quantum efficiency of ca. 0.4 at 298 K. For comparison, the calculated radiative rate constant reported for ABCO is 2.9×10^6 s^{-1}.[14]

For the purpose of analyzing the k_M data, we assume that for ABCH k_{fM} is 3×10^6 s^{-1} and temperature independent. There is no evidence to suggest that the absorption strength of the $S_1 \leftarrow S_0$ transition is temperature dependent; there is a prominant 0–0 band (231.6 nm, see Figure 1) and thus the transition is not vibronically induced. An Arrhenius plot of k_{iM} thus obtained is linear, having an activation energy of 6.5 kJ (540 cm^{-1}). It is also shown in Figure 3. Information about the temperature dependence of nonradiative decay in gas-phase saturated amines is lacking, thus limiting speculation about the mechanism of nonradiative decay in ABCH. It is possible, however, that the cage strain imposed by the methylene bridge presents a channel for photolytic decomposition.

It is significant that k_{DM} manifests a negative temperature dependence (see Figure 3). Although values above 453 K increase slightly, below this temperature, they unequivocally decrease. When analyzed between 298 and 453 K, k_{DM} has an "activation energy" of −10 kJ/mol. This finding implies that excimer formation involves a pre-equilibrium between excited- and ground-state amines. The generation of an excimeric species capable of developing an appreciable emission probability is thus favored by less energetic collisions. The significance of this result will be discussed below in the context of excimer dissociation.

A comparison of k_{DM} with the gas kinetic bimolecular rate constant is enlightening. As usual, however, the problem is to obtain a value of the collision cross section for excimer formation. Because the van der Waals radius of ABCH is not known, we take its collision diameter to be twice the molecular dimension based on the structure of norbornane; this value is ca. 7 Å. To arrive at a reasonable estimate of the collision diameter of the S_1 state of ABCH, we have added 4 Å to this value in order to account for the extensive increase in the size of the nitrogen 3s orbital.[15,16] With use of a mean collision diameter of 9 Å for an excimer-forming encounter between A and A*, a hard sphere rate constant of 6×10^{11} M^{-1} s^{-1} at 298 K is obtained. This implies an excimer formation efficiency of 0.12, when compared with k_{DM} measured at this temperature (6.9×10^{10} M^{-1} s^{-1}). When the same mean collision diameter for excimer formation in ABCO is used, an efficiency of 0.06 is obtained, based on the reported value of k_{DM} for this amine at 299 K (3.1×10^{10} M^{-1} s^{-1}).[4] The higher formation probability for the ABCH excimer may be related to its somewhat larger binding energy (i.e., 51 kJ/mol vis à vis 42 kJ/mol).[2,10]

Dissociation Dynamics

The primary photokinetic parameters obtained from the monomer and excimer decay curves are λ_1, λ_2, and A. These data are used to determine Y which according to Scheme I is the sum of the two intrinsic excimer decay rate constants, k_D and k_{MD}. The challenge in photokinetic studies is the extraction of k_{MD} from

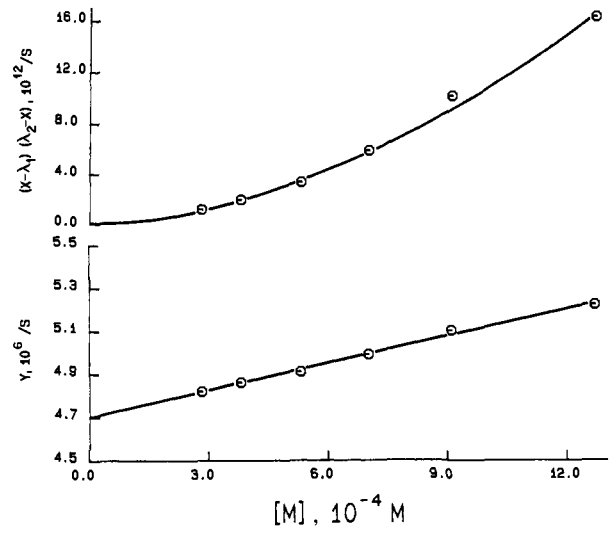

Figure 4. Above: Plot of $(X - \lambda_1)(\lambda_2 - X)$ vs. ABCH vapor concentration at 423 K; the line represents the best fit to eq 8. Below: plot of Y vs. ABCH vapor concentration at 423 K; the line is obtained from linear regression.

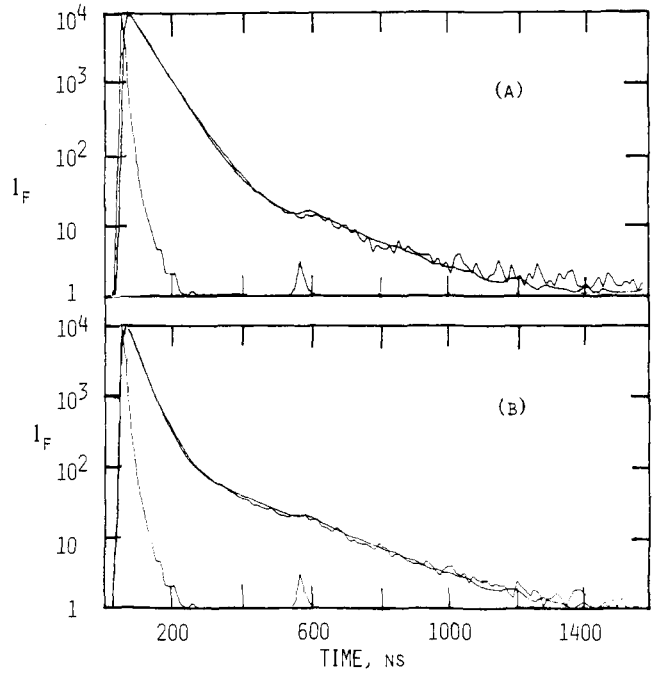

Figure 5. ABCH monomer decay curves at 423 K showing lamp profiles and reconvolutions. Vapor concentration is (a) 3.8×10^{-4} M and (b) 9.1×10^{-4} M.

Y. One approach, based on Scheme I, is to plot the product $\{X - \lambda_1\}\{\lambda_2 - X\}$ vs. [M] (eq 8) and to obtain k_{MD} from the slope ($k_{MD}k_{DM}$), once k_{DM} is determined from the X([M]) data. The

$$\{X - \lambda_1\}\{\lambda_2 - X\} = k_{MD}k_{DM}[M] \qquad (8)$$

intercept of this plot is expected to be zero. It should be noted that in the low-temperture regime, $Y \sim k_D$, and hence $k_D \sim \lambda_1$ (see eq 3 and 5). For ABCH, this places an upper limit on the value of k_D of 3.7×10^6 s^{-1}. It is observed experimentally that λ_1 is temperature independent between 298 and ca. 398 K.

In the high-temperature regime, it is found that Y is weakly concentration dependent, contrary to the expectation manifest by Scheme I. Y vs. [M] is plotted in Figure 4 for data at 423 K. This implies that k_{MD}, k_D, or both rate constants are concentration dependent. Another complication is that plots of eq 8 all clearly show upward curvature; an example is shown in Figure 4 for data at 423 K. This behavior suggests that k_{MD} is concentration dependent. This possibility will be examined in more detail. Model

(13) Reference 9, pp 87–88.
(14) This value, reported in ref 4, is determined from the Strickler–Berg relation. See ref 13.
(15) Köhler, G. *J. Mol. Struct.* **1984**, *114*, 191.
(16) Altenloh, D. D.; Ashworth, L. R.; Russell, B. R. *J. Phys. Chem.* **1983**, *87*, 4348 and references cited therein.

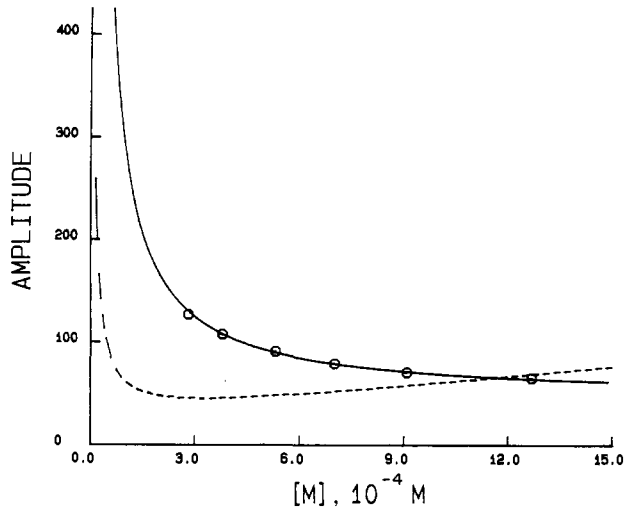

Figure 6. Relative amplitude of the short component in the monomer decay curve, A, vs. ABCH vapor concentration at 423 K: (---) calculated by using Scheme I; (—) calculated according to Scheme I as modified by eq 9; (O) experimental data.

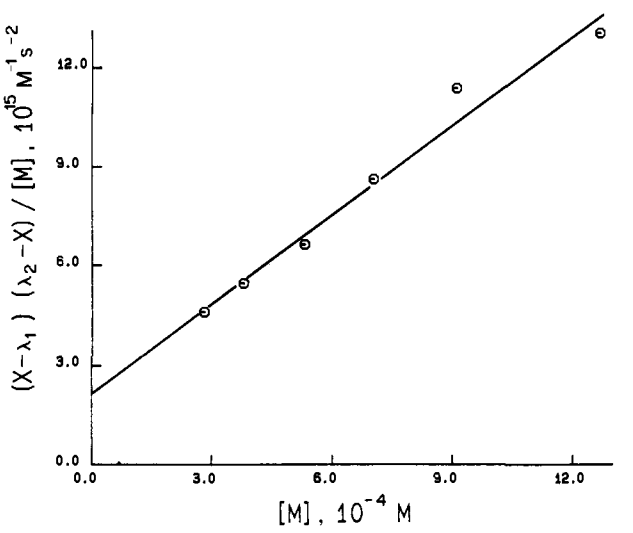

Figure 7. Plot of $(X-\lambda_1)(\lambda_2-X)/[M]$ vs. [M] at 423 K. The linear regression line is used to obtain k_{MD}^0 and k_{MD}' (see Table I).

calculations based on eq 3–5 show that this curvature is associated with the trend in the observed concentration dependence of A, the amplitude of the long-lived component in the monomer decay. Data at 423 K will be used as an example. These data show that A increases with increasing [M] as shown in Figures 5 and 6, which depict respectively two monomer decay curves at different ABCH vapor concentrations and a plot of A vs. [M]. Calculations based on reasonable estimates of the relevant rate constants at this temperature show the opposite trend, also shown in Figure 6. Values of k_M and k_{DM} used in this analysis, obtained from X vs. [M] plots are 1.15×10^7 s^{-1} and 2.1×10^{10} M^{-1} s^{-1}, respectively. Y was partitioned into k_D and k_{MD} by assuming that k_D is temperature independent (i.e., 3.7×10^6 s^{-1}) and that hence $k_{MD} = 1 \times 10^6$ s^{-1} (see Table I).

Mechanistically, the decrease in A with increasing [M] indicates that feedback of excimer into excited monomer becomes more efficient (i.e., faster relative to the intrinsic excimer decay rate) at higher ABCH concentrations. If k_D were concentration dependent, λ_1 would also increase with higher vapor concentrations. This is not observed; hence, we attribute the Y concentration dependence exclusively to k_{MD}. The simple model described by Scheme I was therefore modified by incorporating a concentration-dependent term in the expression of k_{MD}, i.e.

$$k_{MD} = k_{MD}^0 + k_{MD}'[M] \quad (9)$$

where k_{MD}^0 represents the unimolecular dissociation rate constant of the excimer in the zero pressure limit, and k_{MD}' is the bimolecular rate constant accounting for the collisionally induced dissociation of excimer into excited- and ground-state monomers. This modified scheme predicts that $\{X-\lambda_1\}\{\lambda_2-X\}/[M]$ vs. [M] should be linear, having a slope and intercept of $k_{MD}'k_{DM}$ and $k_{MD}^0k_{DM}$, respectively. This mechanism appears to be justified, for the 423 K data shown in Figure 7 are linear with [M] when rendered in this way. Values of k_{MD}^0 and k_{MD}' obtained from this plot are 1.0×10^5 s^{-1} and 4.3×10^8 M^{-1} s^{-1}, respectively. The values obtained at other temperatures are presented in Table I. Consistent with the modified, concentration-dependent k_{MD} is the fact that A, when calculated from eq 5 and 9 and the rate constants cited above, closely follows the experimentally observed values (see Figure 6). It should also be noted that this treatment of k_{MD} is consistent with the observed concentration dependence of Y (see Figure 4), i.e., k_{MD}' is close in value to the slope of Y vs. [M].

This analysis of k_{MD} allows a zero-pressure value of k_D to be obtained from $Y^0 - k_{MD}^0$, where Y^0 is the intercept of Y vs. [M]. These results are also listed in Table I. k_D, when obtained in this way between 398 and 473 K, is temperature dependent. It is interesting that below ca. 398 K where $\lambda_1 \sim k_D$, this rate constant is nearly temperature independent. This suggests that at very low pressures, the spontaneous dissociation of the excimer into excited- and ground-state monomers (the process denoted by k_{MD}^0) is in competition with another unimolecular step above ca. 400 K which does not produce excited-state monomers and may correspond to nonradiative decay, such as $D^* \rightarrow 2M$.

The concentration dependence of k_{MD} can be interpreted in the context of simple unimolecular rate theory (e.g., the Lindemann mechanism[17]) which predicts that collisional energization manifests bimolecular decomposition kinetics at low pressures. According to this model, the measured rate constant should approach zero in the limit of zero pressure and level off to a constant at high pressures. According to this model, the measured rate constant should approach zero in the limit of zero pressure and level off to a constant at high pressures. Assuming that this model has relevance to the ABCH excimer, the failure to observe a leveling off of k_{MD} indicates that our experimental conditions (ABCH vapor only; $P_{max} \sim 30$ Torr) do not extend to high enough pressures (no buffer gas is used).

N_2O_4 provides a good analogy for the ABCH excimer because both compounds involve the unimolecular dissociation of a weak bond (54 kJ in the case of N_2O_4;[18] 51 kJ for $(ABCH)_2$*). For N_2O_4, the fission into NO_2 fragments does not kinetically approach the pseudo-first-order regime until several atmospheres (rather than ca. 1 Torr, as expected for a 6-atom molecule),[19] thus the dissociation is observed to be second order.

Our data indicate that, contrary to the prediction of the Lindemann mechanism (and what is observed for N_2O_4),[20] the dissociation rate constant of the ABCH excimer remains finite in the limit of zero pressure ($k_{MD} \neq 0$, see above). This is probably because the nascent excimer possesses considerable internal energy (i.e., 51 kJ, its binding energy), and, while some of this energy might be rapidly shifted to other internal degrees of freedom, a sufficient amount may remain localized in the N–N excimer bond (over a time scale of tens of hundreds of ns), thus corresponding to an energized species. Apparently the N–N vibrational mode is isolated relative to the other, higher frequency modes in the saturated cage structures. The dissociation rates of the excimer in the zero-pressure limit are very small (10^4–10^5 s^{-1}) and are appreciably increased by energizing collisions with ground-state ABCH (see eq 8). It is noteworthy in this context that the fluorescence enhancement of the ABCO and ABCH excimers as a result of vibrational relaxation has been observed.[4,11] We also note that the negative temperature coefficient observed for the

(17) Moore, J. W.; Pearson, R. G. *Kinetics and Mechanism*, 3rd ed.; Wiley: New York, 1981; pp 122–126.
(18) Verhoek, F. H.; Daniels, F. *J. Am. Chem. Soc.* **1931**, *53*, 1250.
(19) Benson, S. W. *Foundations of Chemical Kinetics*; McGraw-Hill: New York, 1960; pp 260–261.
(20) Carrington, T.; Davidson, N. *J. Phys. Chem.* **1953**, *57*, 418.

formation rate constant, k_{DM} (see above), is consistent with a reversible fission reaction which takes place in the low-pressure regime.

The Lindemann mechanism discussed above is often associated with the Hinshelwood rate constant, k_{df}, which accounts for collisional activation exploiting vibrational degrees of freedom. It is interesting therefore to compare the value of k_{MD}' with that obtained from the Hinschelwood formulation[21] which is

$$k_{df} = k_{hs}\{E_0/RT\}^{(s-1)}\{(s-1)!\}^{-1}\exp(-E_0/RT) \quad (10)$$

where k_{hs} is the hard sphere bimolecular rate constant, E_0 is the critical energy (i.e., excimer binding energy), and s is the effective number of oscillators in the molecule promoting collisional energization. At 423 K, $k_{MD}' = 4.5 \times 10^8$ M^{-1} s^{-1}, and taking E_0 to be 50 kJ, the condensed phase binding energy, a value of s = 4 is required in eq 10. This compares with s = 5, cited by Carrington and Davidson for N_2O_4.[20] It is, perhaps, striking that in a much larger molecule such as the ABCH excimer a similar number of effective oscillators is implicated in collisional energization.

The interpretation of the temperature dependence of k_{MD}^0 is not straightforward. These rate constants do not represent a system at thermal equilibrium and hence the parameters obtained from an Arrhenius plot would not be expected to correspond to thermodynamic quantities; for example, the observed activation energy of k_{MD}^0 would be expected to be less than that of the excimer bond strength. At moderate pressures where dissociation is second order (the fall-off region), the observed activation energy is predicted to be less than the critical energy, E_0, by an amount $(s - 3/2)RT$.[22] For s = 4, this difference is ca. 9 kJ/mol at 423 K. An Arrhenius plot of k_{MD}^0 between 398 and 473 K is curved and thus it is probably not meaningful to extract an activation energy from these data, although the slope (obtained from linear regression) is 24 kJ/mol. This is considerably less than that predicted (41 kJ/mol).

A brief comment about the feasibility of studying the ABCH monomer/excimer system at higher total pressures is in order. These experiments, while important to pursue, are difficult to carry out. First, the kinetics of mixing between the buffer gas and ABCH is an issue that represents a particular experimental challenge. Second, there is the serious complication that the administration of even moderate pressures of chapeyron gases causes significant changes in the excited monomer rate parameter, k_M. Data reveal that both the radiative and nonradiative rate constants of excited-state amines increase as a result of collisions with N_2 or CH_4;[23] hence, one apparently deals with a different photophysical system (and scheme) for each buffer gas environment.

Photostationary Measurements

As a check of the mechanism proposed above, as well as the rate constants and their temperature dependences, photostationary measurements were made of the ABCH system for vapor temperatures between 298 and 473 K. Monomer and excimer fluorescence intensities (I_{fM} and I_{fD}) were monitored at 256 and 380 nm, respectively. The ABCH vapor concentration was constrained to be 2.35×10^{-3} M, i.e., within the range of values used in the photokinetic studies. In order to keep this concentration constant despite the changing vapor temperature, the vapor pressure was adjusted accordingly by controlling the temperature of the solid contained in the cell sidearm (see Experimental Section).

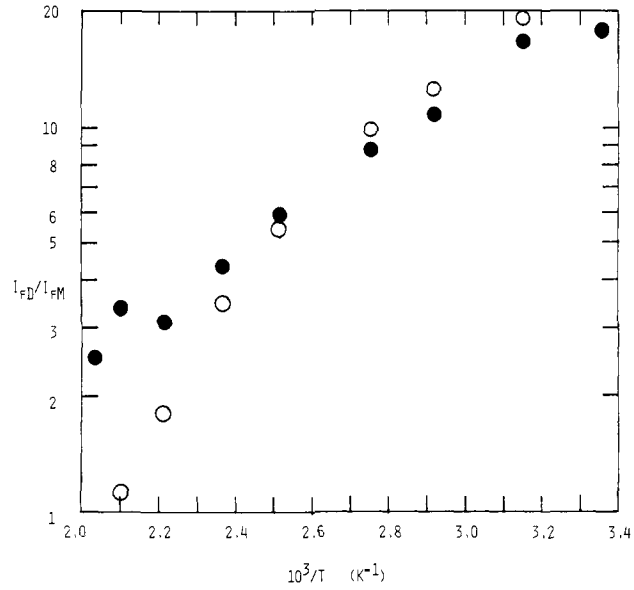

Figure 8. Arrhenius plots of I_{fD}/I_{fM} determined from photostationary measurements (○) and photokinetic data, k_{DM}/Y (●). The photostationary ratios are arbitrarily normalized to the photokinetic results.

These results are compared with the photokinetic dta through the following equation

$$I_{fD}/I_{fM} = (k_{fD}/k_{fM})(k_{DM}[M]/Y) \quad (11)$$

where the rate constants are defined in eq 4, 6, and 9. The photostationary and kinetic data are in general agreement with each other. This is demonstrated in Figure 8, which contains an Arrhenius plot of (11) along with the measured intensity ratios. The photostationary data are arbitrarily normalized relative to the ratio k_{DM}/Y. The $k_{fD}[M]/k_{fM}$ term is treated as a constant. It appears that the photostationary data curve downward more sharply at higher temperatures than the photokinetic results, possibly indicating temperature dependence of k_{fD} and or k_{fM} in this regime.

Conclusions

Vapor-phase excimer formation in ABCH can be observed and studied photokinetically. Evidence of thermal dissociation of the excimer into excited- and ground-state monomers cannot be obtained photokinetically at temperatures below ca. 400 K because of the very small value of the rate constant ($<10^4$ s^{-1}). Above that temperature, fission of the excimer appears to proceed as a bimolecular process, even at ABCH pressures as high as 30 Torr; hence, the true unimolecular rate constant cannot be directly determined. Consistent with excimer dissociation being observed within the "falloff" region is the observation that the formation rate constant has a negative activation energy. On the basis of a hard sphere collision model in which a mean collision diameter of 9 Å is used, the net efficiency of emissive excimer formation is ca. 0.12.

Acknowledgment. The authors are grateful to the donors of the Petroleum Research Fund, administered by the American Chemical Society, for partial support of this work.

Registry No. 1-Azanorbornane, 279-27-6.

(21) Reference 17, pp 126–127.
(22) Reference 19, pp 234–239.
(23) Halpern, A. M.; Zhang, X. K.; Taaghol, A., unpublished results.